

Dysregulation of intracellular pH is a cause of impaired capacitation in Slc22a14-deficient mice

メタデータ	言語: eng 出版者: 公開日: 2021-10-28 キーワード (Ja): キーワード (En): 作成者: Ito, Momoe, Unou, Masato, Higuchi, Toshiya, So, Shuhei, Ito, Masahiko, Yogo, Keiichiro メールアドレス: 所属:
URL	http://hdl.handle.net/10297/00028410

1 **Dysregulation of intracellular pH is a cause of impaired capacitation in *Slc22a14*-deficient mice**

2
3 Momoe Ito¹, Masato Unou², Toshiya Higuchi¹, Shuhei So^{3,4}, Masahiko Ito⁵, and Keiichiro Yogo^{1,2,6}

4
5 ¹Department of Applied Life Sciences, Faculty of Agriculture, Shizuoka University, Shizuoka, Japan

6 ²Department of Agriculture, Graduate School of Integrated Science and Technology, Shizuoka
7 University, Shizuoka, Japan

8 ³Department of Reproductive and Perinatal Medicine, Hamamatsu University School of Medicine
9 Shizuoka Japan

10 ⁴Tawara IVF Clinic, Shizuoka, Japan

11 ⁵Department of Virology and Parasitology, Hamamatsu University School of Medicine, Hamamatsu,
12 Shizuoka, Japan.

13 ^{1,2,6}College of Agriculture, Academic Institute, Shizuoka University, Shizuoka, Japan

14
15 Keywords: bicarbonate, capacitation, intracellular pH, sperm, transporter

16
17 Short title: Mechanism of impaired sperm capacitation

18
19 Corresponding author: Keiichiro Yogo, Ph.D. Associate Professor

20 Laboratory of Gene function in Animals, College of Agriculture, Academic Institute, Shizuoka

21 University

22 836 Ohya, Suruga, Shizuoka 422-8529 Japan

23 E-mail: yogo.keiichiro@shizuoka.ac.jp

24
25 Word count of full article: 4940 words

26 **Abstract**

27 Solute carrier 22a member 14 (SLC22A14) plays a critical role in male infertility in mice. We
28 previously revealed that one of the causes of infertility is impaired capacitation. However, the
29 molecular mechanism remained unclear. Here, we show that the influx of HCO_3^- , a trigger of
30 capacitation, is impaired and intracellular pH is decreased in the sperm of *Slc22a14* knockout (KO)
31 mice. While intracellular cAMP concentration did not increase during capacitation in *Slc22a14* KO
32 spermatozoa, HCO_3^- -dependent soluble adenylyate cyclase activity was normal, and the addition of 8-
33 bromo cAMP rescued the decreased protein tyrosine phosphorylation. In addition, the intracellular pH
34 of *Slc22a14* KO sperm was lower than that of wild-type sperm and did not increase after the addition
35 of HCO_3^- . Although its relationship to the regulation of intracellular pH is unknown, TMEM225, a
36 possible protein phosphatase inhibitor, was found to be decreased in *Slc22a14* KO sperm. The
37 decreased in vitro fertilization rate of *Slc22a14* KO sperm was partially rescued by an increase in the
38 intracellular pH (pHi) and the addition of 8-bromo cAMP. These results suggest that SLC22A14 is
39 involved in capacitation through the regulation of HCO_3^- transport and pHi.

40

41 **Introduction**

42 In mammals, spermatozoa immediately after ejaculation cannot fertilize oocytes. Before
43 fertilization, spermatozoa must spend a certain amount of time in the female reproductive tract. During
44 this process, spermatozoa undergo many physiological and biochemical changes that are necessary for
45 fertilization. For example, sperm display hyperactivated motility characterized by high amplitude and
46 vigorous asymmetrical beating of the tail, and become functionally competent for the acrosome
47 reaction. In addition, reorganization and modification of sperm plasma membrane protein/lipid are
48 induced, which facilitate zona binding or fusion with the oocyte oolemma (Gadella 2008). These
49 collective changes that allow sperm to fertilize eggs in spermatozoa are termed capacitation.

50 The influx of HCO_3^- triggers capacitation. Although cauda epididymal fluid contains low

51 levels of HCO_3^- , spermatozoa get exposed to higher concentrations of HCO_3^- in the seminal plasma
52 and in female reproductive fluids before fertilization (Okamura *et al.* 1985, Liu *et al.* 2012). HCO_3^- is
53 transported to the cytoplasm via transporters. The incorporated HCO_3^- activates soluble adenylyl
54 cyclase (Chen *et al.* 2000) and intracellular cAMP is increased. Subsequently, protein kinase A (PKA)
55 is activated and a series of downstream signaling pathways are activated, which include the protein
56 tyrosine phosphorylation (Visconti *et al.* 1995a, Visconti *et al.* 1995b). In addition, the incorporation
57 of HCO_3^- induces an increase in intracellular pH (pHi). pHi is regulated by Na^+/H^+ exchangers and
58 bicarbonate transporters, and alkalization during capacitation plays an important role in sperm function
59 (Nishigaki *et al.* 2014). For example, Slo3, a potassium channel that is involved in membrane
60 depolarization and is essential in sperm motility and male fertility (Zeng *et al.* 2011), is activated by
61 increased pHi (Schreiber *et al.* 1998). Similarly, CatSper, a Ca_2^+ channel that is essential for
62 hyperactivated motility and male fertility (Ren *et al.* 2001), is activated by increased pHi and
63 membrane depolarization (Kirichok *et al.* 2006). However, the molecular nature of HCO_3^- transporters
64 and their regulatory mechanisms are unclear.

65 Solute carrier 22a member 14 (SLC22A14) is an organic cation/anion/zwitterion transporter.
66 Recently, we described that SLC22A14 is pivotal in male fertility (Maruyama *et al.* 2016). SLC22A14
67 is expressed specifically in male germ cells in mice and is localized in the principal piece of sperm.
68 *Slc22a14* knockout (KO) mice show reduced sperm motility due to abnormal flagellar bending caused
69 by osmotic cell swelling and structural abnormalities in the annulus. In addition, capacitation was
70 impaired in *Slc22a14* KO sperm, as evidenced by the lack of an increase in protein tyrosine
71 phosphorylation (a marker for capacitation in sperm). Owing to these abnormalities, *Slc22a14* KO
72 male mice show severe infertility. However, the mechanism of impaired capacitation in these mice has
73 been unclear. In this study, we investigated the signaling cascade of capacitation and differentially
74 expressed proteins in *Slc22a14* KO sperm.

75

76 **Materials and methods**

77 *Animals and ethical considerations*

78 The wild-type (WT) and *Slc22a14* KO mice (C57BL/6N strain) and genotyping of mice
79 were performed as previously described (Maruyama *et al.* 2016). We used mice aged 8 weeks to 8
80 months, which is generally considered to be the extent of their reproductive period. We used age-
81 matched (\pm 1 month) wild-type and KO mice in each experiment. All animal experiments were
82 approved by the Institutional Committees for Experimental Animal Care and Use of Shizuoka
83 University and were conducted in accordance with the guidelines of the institution. Unless otherwise
84 noted, we compared sperm between genotypes, using one mouse of each genotype per iteration of our
85 experiment.

86

87 *Sperm collection*

88 The cauda epididymis was removed from each male mouse and partially incised using
89 scissors. The tissues were transferred to TYH medium (119.37 mM NaCl, 4.78 mM KCl, 1.71 mM
90 $\text{CaCl}_2 \cdot 2\text{H}_2\text{O}$, 1.19 mM KH_2PO_4 , 1.19 mM $\text{MgSO}_4 \cdot 7\text{H}_2\text{O}$, 5.56 mM glucose, 25.07 mM NaHCO_3 , 1
91 mM Na-pyruvate) supplemented with 4 mg/mL bovine serum albumin (BSA). Sperm were gently
92 pushed out using tweezers under a stereomicroscope and incubated at 37°C. When sperm were
93 collected under non-capacitating conditions, NaHCO_3 -free HEPES-buffered TYH medium without
94 BSA (TYH-HEPES, pH 7.4) was used.

95

96 *Measurement of intracellular cAMP level*

97 Cauda epididymal sperm were released into TYH-HEPES medium and incubated for 30 min
98 at 37°C. The sperm suspensions were transferred to 1.5 mL tubes and incubated in the presence or
99 absence of NaHCO_3 and BSA (final concentrations were 25.07 mM and 4 mg/mL, respectively) for 0
100 to 30 min at 37°C. The reaction was stopped by the addition of 1N HCl and 10% v/v Triton X-100

101 (final concentrations were 0.1 M and 1% v/v, respectively). The lysates were centrifuged at $17,000 \times$
102 g for 20 min, and the supernatants were stored at -80°C . Intracellular cAMP levels were measured
103 using a direct cAMP assay kit (Enzo Life Sciences, East Farmingdale, NY, USA) according to the
104 manufacturer's instructions. Briefly, samples and standard solutions were added to wells coated with
105 secondary antibody, followed by anti-cAMP antibody and competitive alkaline phosphatase-
106 conjugated cAMP. After 2 h of incubation with shaking, the wells were washed and substrate solution
107 (*p*-nitrophenyl phosphate) was added. After 1 h incubation at room temperature, the reactions were
108 stopped and absorbance at 405 nm was measured using a Varioskan LUX microplate reader (Thermo
109 Fisher Scientific, Waltham, MA, USA). The concentration of cAMP was calculated using a standard
110 curve.

111

112 *Measurement of soluble adenylate cyclase activity in vitro*

113 Soluble adenylate cyclase activity was measured in vitro using previously reported methods
114 (Jaiswal & Conti 2001, Wang *et al.* 2007). The cauda epididymal spermatozoa collected in TYH-
115 HEPES medium were washed with PBS by centrifugation. The pellets were resuspended in
116 homogenization buffer (50 mM Tris-Cl [pH 7.4], 5 mM MnCl_2 , 1 mM EDTA, 1 mM dithiothreitol
117 [DTT], 1 mM phenylmethylsulfonyl fluoride [PMSF]), disrupted by sonication, and centrifuged at
118 $14,000 \times$ g for 20 min at 4°C . The supernatants were collected and centrifuged again at $100,000 \times$ g
119 for 20 min at 4°C . Each supernatant (cytosol fraction) was used for the following assay. The protein
120 concentration of the lysate was measured by the BCA method and diluted with homogenization buffer
121 to $0.22 \mu\text{g}/\mu\text{L}$. Then, 90 μL of lysate (20 μg protein) and an equal volume of reaction buffer (50 mM
122 Tris-Cl [pH 7.4], 5 mM MnCl_2 , 2 mM ATP, 20 mM phosphoenol pyruvate, 6 units pyruvate kinase,
123 0.4 mM IBMX) were mixed and incubated for 20 min at 37°C with or without 100 mM NaHCO_3 . The
124 reaction was stopped by the addition of 20 μL of 1 N HCl and cAMP concentrations were measured
125 as described above.

126

127 *Measurement of pHi*

128 The pHi was measured as previously reported (Demarco *et al.* 2003). Briefly, the cauda
129 epididymal spermatozoa were collected in TYH-HEPES and charged with the pH-sensitive dye 2',7'-
130 bis-(2-carboxyethyl)-5-(and-6)-carboxyfluorescein (BCECF-AM; final concentration 4 μ M) for 15
131 min at 37°C. Sperm (5×10^6) were washed three times with TYH-HEPES, moved to a cuvette, and
132 incubated at 37°C for 0, 1, 5, 15, or 30 min in the presence or absence of NaHCO₃ and BSA (final
133 concentration 25.07 mM and 4 mg/mL, respectively). The emitted fluorescence at 540 nm following
134 excitation at 440 nm and 500 nm was measured using a model FP-6500 fluorescence
135 spectrophotometer (JASCO Corporation, Tokyo, Japan). For pH calibration, BCECF-charged
136 epididymal sperm were washed three times in TYH-HEPES having different pH values (6.0, 6.5, 7.0,
137 and 7.5) and permeabilized with 0.1% v/v Triton X-100. The fluorescence intensities of each sample
138 were measured. The pHi in each condition was calculated using a standard curve constructed from the
139 graph plotted with the ratio of fluorescence intensity (500/440) and pH.

140

141 *Isobaric tags for relative and absolute quantitation analysis (iTRAQ) analysis*

142 The cauda epididymal spermatozoa were collected and washed three times with ice-cold
143 PBS. Sperm suspension (approximately 4×10^7 cells) was transferred to low protein-binding
144 microcentrifuge tubes and mixed with four times the volume of ice-cold acetone. After several
145 inversions, the tubes were stored at -20°C for 3 h and centrifuged at 12,000 \times g for 20 min. Each
146 supernatant was discarded, and the pellet was dissolved in 20 mM HEPES (pH 8.5) buffer containing
147 8 M urea, 4% v/v CHAPS, 20 μ M EDTA, 100 μ M DTT, and a protease inhibitor cocktail (Sigma-
148 Aldrich). St. Louis, MO, USA). After centrifugation at 17,000 \times g for 20 min, the supernatant was
149 transferred to a new tube, mixed with cold acetone, and stored at -20°C overnight. The precipitated
150 proteins were recovered by centrifugation, dried, and dissolved in 0.5 M triethylammonium

151 bicarbonate (TEAB; Sigma-Aldrich). Low molecular weight (< 3,000) substances were removed using
152 an Amicon Ultra Centrifugal Filter Unit (Millipore, Billerica, MA, USA). Protein concentrations were
153 determined using a BCA protein assay kit (Pierce, Rockford, IL, USA). One hundred micrograms of
154 protein was reduced with 0.05 M tris-(2-carboxyethyl) phosphine (TCEP), alkylated with 0.2 M
155 methyl methane-thiosulfonate, and digested with TPCK-trypsin (w/CaCl₂; Sigma-Aldrich). The
156 peptides were labeled with iTRAQ Reagents Multiplex Kit (AB Sciex, Framingham, MA, USA)
157 according to the manufacturer's instructions. To remove all interfering substances, strong cation
158 exchange chromatography was performed for the combined iTRAQ-labeled peptides using the cation
159 exchange system provided in the iTRAQ Method Development Kit (AB Sciex). The eluted fraction
160 was desalted using Sep-Pak C18 cartridges (Waters, Milford, MA, USA), dried, and reconstituted with
161 100 µL of 0.1% v/v formic acid. The peptides were analyzed using a Q Exactive Hybrid Quadrupole-
162 Orbitrap Mass Spectrometer (Thermo Fisher Scientific) with Xcalibur (version 2.2). Proteome
163 Discoverer software (version 2.0; Thermo Fisher Scientific) was used to generate peak lists from raw
164 MS data files. To identify the peptides, the resulting peak lists were submitted to a SEQUEST search
165 engine (Thermo Fisher Scientific) and compared against the mouse protein database (SwissProt,
166 release 2018/06). We analyzed protein expression in two WT and two KO samples using 4-plex
167 analysis. Each sample contained proteins from several mice to avoid any individual differences. For
168 analysis of membrane proteins, the membrane fraction of sperm was isolated using the Minute Plasma
169 Membrane Protein Isolation Kit (Invent Biotechnology, Plymouth, MA, USA) and analyzed in a
170 similar way.

171

172 *Semi-quantitative RT-PCR*

173 Total RNA was isolated from mouse testes using ISOGEN (Nippon Gene, Tokyo, Japan),
174 and reverse transcription was performed as previously described (Muroi *et al.* 2017). PCR was
175 performed using the KOD-FX Neo DNA polymerase (TOYOBO, Osaka, Japan). The primer pairs

176 used are listed in Supplementary Table 1. PCR products were electrophoresed in 1.2 or 1.5 % agarose
177 gel and stained with ethidium bromide. Images were captured using a Canon digital camera (SX10IS,
178 Canon, Inc., Tokyo, Japan). The expression levels of the gene between samples were compared during
179 the cycles, which showed that the PCR product increased exponentially. An equal amount of template
180 between the samples was confirmed using glyceraldehyde 3-phosphate dehydrogenase (GAPDH).

181

182 *Western blotting*

183 SDS-PAGE and western blotting were performed according to standard protocols. The testes
184 were homogenized in 1% Triton X-100 lysis buffer (50 mM Tris-Cl pH 7.4, 150 mM NaCl, 2 mM
185 EDTA, 2 mM phenylmethylsulfonyl fluoride, 2 mM Na₃VO₄, 20 mM NaF, and 1% Triton X-100) and
186 the lysates were centrifuged at 17,000 × g for 20 min at 4°C. The supernatant was transferred to
187 microtubes, mixed with an equal volume of 2× sample buffer (125 mM Tris/sodium dodecyl sulfate
188 [SDS] (pH 6.8), 4% w/v SDS, 20% v/v glycerol, 10% v/v 2-mercaptoethanol, and 0.002% w/v
189 bromophenol blue), and incubated at 100°C for 5 min. In the analysis of TMEM225 expression,
190 TMEM225 was immunoprecipitated from testis lysate (300 µg protein) with anti-TMEM225 antibody
191 (Matsuura & Yogo 2015) and resuspended in 2× sample buffer. Sperm were incubated in TYH medium,
192 washed with PBS, and resuspended in 2× sample buffer. In the tyrosine phosphorylation rescue
193 experiments, 0.5 mM 8-bromo-cAMP and 50 µM 3-isobutyl-1-methylxanthine (IBMX) were added to
194 the medium. The proteins were separated by 7.5%, 10%, or 12.5% acrylamide gel electrophoresis,
195 transferred onto a polyvinylidene difluoride membrane, and detected by western blotting. The
196 following primary antibodies were used: anti-phospho-tyrosine antibody (clone 4G10 from Merck,
197 Kenilworth, NJ, USA or GeneTex, Inc., Irvine, CA, USA), anti-GAPDH antibody (FUJIFILM Wako
198 Pure Chemical Corporation, Osaka, Japan), anti-SLC26A3 (Santa Cruz Biotechnology, Dallas, TX,
199 USA), and anti-SLC26A6 (Santa Cruz Biotechnology). Anti-TMEM225 antibodies have been
200 described previously (Matsuura & Yogo 2015, Maruyama *et al.* 2016). Horseradish peroxidase (HRP)-

201 conjugated anti-rabbit IgG and anti-mouse IgG secondary antibodies were purchased from SeraCare
202 (Milford, MA, USA). For IP-western blotting, HRP-conjugated protein-A (BioLegend, San Diego,
203 CA, USA) was used to prevent the detection of IgG used for IP. Signals were visualized using
204 homemade ECL solution (Haan & Behrmann 2007) or ECL Prime (Cytiva, Marlborough, MA, USA).
205 The images of the X-ray photos were captured by a model GT-6500 image scanner (Epson, Nagano,
206 Japan). The quantification of band intensity was performed using Image J software (Schneider *et al.*
207 2012), and the expression levels of target proteins were normalized to GAPDH.

208

209 *In vitro fertilization*

210 In vitro fertilization was performed as previously described, with slight modifications
211 (Maruyama *et al.* 2016). ICR female mice (8–12 weeks old) were injected with 7.5 IU pregnant mare
212 serum gonadotropin (PMSG) and 7.5 IU human chorionic gonadotropin (hCG) at 48 h intervals.
213 Cumulus-oocyte complexes were collected 16 h after injection of hCG from the oviduct ampulla and
214 moved to a 100 µl drop of TYH medium covered with mineral oil (Nacalai Tesque, Inc., Kyoto, Japan).
215 Cauda epididymal spermatozoa were released into a 200 µl drop of TYH medium and incubated in a
216 CO₂ incubator at 37°C for 60 min before fertilization. Depending on the group, the TYH medium
217 supplemented with 10 mM trimethylamine (TMA) hydrochloride, 0.5 mM 8-bromo cAMP, or 0.05
218 mM IBMX was used. Spermatozoa were then incubated with oocytes at a concentration of 5×10⁵/ml.
219 A portion of the remaining sperm was used for assessment of motility and morphology, as described
220 below. After 4 h, the oocytes were washed, transferred to M16 medium supplemented with antibiotic-
221 antimycotic solution (FUJIFILM Wako Pure Chemical Corporation, Osaka, Japan), and cultured in a
222 CO₂ incubator at 37°C. The number of 2-cell embryos were counted 24 h after insemination.

223

224 *Assessment of sperm motility and morphology*

225 A portion of the sperm suspension (10–20 µl) incubated in TYH medium for 60 min was

226 spotted onto glass slides and covered with cover glass. The corners of the cover glass was rested on
227 spots of a Vaseline-paraffin mixture, providing space for the sperm to swim freely. The motility of
228 sperm was manually categorized into three groups (highly motile with progressive motility, motile but
229 with weak or no progressive motility, and immotile), and the percentage of sperm in the category was
230 determined by observation using an Olympus IX70 microscope (Olympus Corporation, Tokyo, Japan).
231 Another portion of the sperm suspension was mixed with 3.8% paraformaldehyde for fixation,
232 smeared on glass slides, and mounted in 50% glycerol/PBS. The number of sperms with normal or
233 abnormal flagellar bending (hairpin type and V-shape type) were counted under a microscope.

234

235 *Statistical Analysis*

236 Statistical analyses of the data were performed using one-way analysis of variance with Tukey's
237 multiple comparison post-hoc test. Statistical significance was set at $p < 0.05$.

238

239 **Results**

240 *cAMP production is impaired in Slc22a14 KO sperm*

241 We first confirmed impaired capacitation in *Slc22a14* KO mice. WT and *Slc22a14* KO
242 spermatozoa were incubated in capacitation conditions for 5 to 90 min, and protein tyrosine
243 phosphorylation was monitored by western blotting. The protein phosphorylation level was increased
244 during the incubation period in WT sperm, whereas that of KO sperm was not prominent (Fig. 1A and
245 1B), as previously reported (Maruyama *et al.* 2016). This result suggests that the signaling cascade of
246 capacitation is not induced or delayed in KO sperm.

247 Next, we investigated the changes in intracellular cAMP concentration during capacitation.
248 In WT sperm, cAMP concentration increased rapidly at one min after the addition of HCO_3^- and
249 decreased to basal levels at 5 min. Thereafter, cAMP concentration increased again gradually to 30
250 min, as reported previously (Wang *et al.* 2007). In contrast, the rapid increase in cAMP was not

251 significant in *Slc22a14* KO sperm, and an increase in the later phase was not observed (Fig. 2).

252

253 *Soluble adenylyl cyclase activity and its downstream signaling are normal in Slc22a14 KO sperm*

254 One possible explanation for the foregoing results is that soluble adenylyl cyclase activity
255 is reduced in *Slc22a14* KO sperm. To explore this, we examined cAMP production in vitro using the
256 cytosolic fraction of sperm. No difference was evident between WT and KO mice in the presence or
257 absence of HCO_3^- (Fig. 3). This result indicated that HCO_3^- -dependent soluble adenylyl cyclase is
258 intact in *Slc22a14* KO sperm. We further examined the effect of cell-permeable cAMP on protein
259 tyrosine phosphorylation. As shown in Fig. 4, the addition of 8-bromo-cAMP and IBMX
260 (phosphodiesterase inhibitor) almost completely rescued the reduced protein tyrosine phosphorylation
261 in *Slc22a14* KO sperm. This result suggested that the signaling cascade downstream of cAMP is
262 normal, but that the influx of HCO_3^- is impaired in *Slc22a14* KO sperm. However, when only 8-
263 bromo-cAMP was added, the recovery of tyrosine phosphorylation was approximately 50% (data not
264 shown). Thus, we cannot exclude the possibility that phosphodiesterase activity is higher in *Slc22a14*
265 KO sperm.

266

267 *pHi does not increase in the capacitation condition in Slc22a14 KO sperm*

268 To investigate the influx of HCO_3^- , we monitored changes in pHi in sperm before and after
269 the addition of HCO_3^- using BCECF-AM. In the absence of HCO_3^- , the pHi of WT sperm was $6.91 \pm$
270 0.03 . The pHi gradually increased after the addition of HCO_3^- and reached 7.19 ± 0.03 after 30 min
271 (Fig. 5). The change in pHi was not in accordance with the change in intracellular concentration of
272 cAMP (Fig. 2). The reason for this is not clear, but it is possible that pHi is regulated by factors other
273 than the influx of HCO_3^- or that phosphodiesterase activity is higher immediately after the start of
274 capacitation. In contrast, the pHi of *Slc22a14* KO sperm was lower than that of WT sperm in the
275 absence of HCO_3^- (6.77 ± 0.01), and it did not increase with the addition of HCO_3^- (Fig. 5). This result

276 suggested that the expression or function of the transporter(s) that regulate pHi is impaired in *Slc22a14*
277 KO mice.

278

279 *iTRAQ analysis in Slc22a14 KO mice*

280 Next, we investigated the expression of ten transporters involved in HCO₃⁻ or H⁺ transport
281 using RT-PCR or western blotting, if specific antibodies were available. These transporters are known
282 or predicted to be involved in male fertility or sperm capacitation. The expression levels of the
283 transporters in *Slc22a14* KO mice testes were comparable to those in WT mice (Supplementary Figure
284 1). Thus, we searched more comprehensively for differentially expressed proteins in *Slc22a14* KO
285 sperm using iTRAQ. An analysis using total sperm protein revealed that only myosin light chain 6 B
286 as was a differentially expressed protein (> two-fold change) out of a total of 719 identified proteins.
287 SLC transporters were not included in 719 proteins (Supplementary Figure 2). Therefore, we
288 performed iTRAQ using the membrane fraction of spermatozoa to more efficiently identify
289 transporters. A total of 670 proteins were identified, which was comparable to previous iTRAQ
290 analysis using bovine sperm (D'Amours *et al.* 2019). The membrane protein content was
291 approximately 70%. In the membrane fraction analysis, 13 proteins were identified as downregulated
292 in *Slc22a14* KO sperm, whereas no upregulated proteins were identified. These included
293 transmembrane protein 225 (TMEM225), carcinoembryonic antigen-related cell adhesion molecule
294 10 (CEACAM10), and seminal vesicle secretory protein 5 (SVS5) (Table 1). Although some SLC
295 transporters known to regulate pHi were included in 670 proteins, their expression in KO sperm was
296 comparable to that of WT (Table 2). TMEM225 is expressed specifically in spermatozoa and acts as
297 an inhibitor of protein phosphatase 1 (PP1) (Matsuura & Yogo 2015). In addition, TMEM225 has been
298 classified as an essential gene for male fertility in mice by the International Mouse Phenotype
299 Consortium (IMPC). We confirmed the decreased expression of TMEM225 in KO testes by western
300 blotting (Fig. 6A, 6 B). On the other hand, mRNA expression of *Tmem225* was comparable with that

301 of the WT (Fig. 6C), suggesting that the decreased expression could have been caused by decreased
302 translation efficiency or protein stability.

303

304 *Alkalization of pHi and addition of cAMP partially rescued fertilization rate in Slc22a14 KO sperm*

305 We investigated whether the decreased fertilization rate of *Slc22a14* KO sperm can be
306 recovered by alkalization of pHi and/or addition of cAMP. We selected trimethylamine (TMA), an
307 alkalization agent known to sustain increased pHi (Alasmari *et al.* 2013). In a preliminary experiment,
308 we found that 10 mM TMA increased pHi to 7.08 ± 0.06 in KO sperm (approximately the same level
309 as the WT control, Supplementary Figure 3). As shown in Fig. 7A, the fertilization rate did not increase
310 with the respective addition of 10 mM TMA or 8-bromo cAMP/IBMX to the capacitation medium,
311 but their combination significantly increased fertilization rate compared to the control in *Slc22a14* KO
312 sperm. However, the fertilization rate was apparently lower than that of WT sperm, and the recovery
313 of fertilization ability was limited. Next, we examined the effect of the addition of TMA and
314 cAMP/IBMX on sperm motility and morphology. Decreased motility and abnormal flagellar bending
315 in KO sperm were not rescued by the addition of TMA and cAMP/IBMX (Figs. 7B and 7C). This is a
316 plausible reason for the partial recovery of fertilization ability. Taken together, these results suggest
317 that the addition of TMA and cAMP bypasses the initiation process of capacitation and induces the
318 signaling cascades necessary for fertilization in *Slc22a14* KO sperm, at least in part.

319

320 **Discussion**

321 We previously found that SLC22A14 is necessary for capacitation in mouse sperm
322 (Maruyama *et al.* 2016). However, the underlying mechanism remains to be elucidated. In the present
323 study, we investigated the signaling cascade of capacitation in *Slc22a14* KO mice. Although an
324 increase in cAMP was not observed, the signaling pathway downstream of cAMP was intact in
325 *Slc22a14* KO spermatozoa. The pHi of *Slc22a14* KO sperm was comparatively lower and did not

326 increase during capacitation in *Slc22a14* KO spermatozoa. The addition of an alkalizing reagent and
327 cAMP/IBMX partially rescued the impaired fertilizing ability. These results suggest that impaired
328 influx of HCO_3^- and low pHi are likely causal factors of impaired capacitation in *Slc22a14* KO
329 spermatozoa.

330 The addition of cAMP/IBMX almost completely rescued tyrosine phosphorylation but not
331 the in vitro fertilization rate. This suggests that upregulation of protein tyrosine phosphorylation is not
332 sufficient, and increased pHi-dependent activation processes, such as activation of Slo3 or CatSper,
333 are also required for capacitation in *Slc22a14* KO sperm. Meanwhile, the rescue of decreased
334 fertilizing ability in KO sperm by the addition of TMA and cAMP/IBMX was partial. A likely reason
335 for insufficient recovery would be that the decreased motility and abnormality of flagella were not
336 restored. Considering that abnormal flagellar angulation of *Slc22a14* KO sperm is caused by osmotic
337 cell swelling and annulus disorganization, it is reasonable that flagellar abnormalities could not be
338 relieved by the alkalizing reagent or cAMP.

339 The mechanisms of impaired influx of HCO_3^- and decreased pHi in *Slc22a14* KO sperm
340 were not elucidated in this study. Since no SLC22A family member has been reported to be able to
341 transport HCO_3^- or H^+ , the possibility that SLC22A14 acts as a bicarbonate and/or proton transporter
342 will be excluded. Kuang et. al (Kuang *et al.* 2021) recently reported that SLC22A14 serves as a
343 mitochondrial riboflavin transporter and that metabolites of glycolysis, such as pyruvate and lactate,
344 accumulate in *Slc22a14* KO sperm. Since we have shown in a previous study that SLC22A14 localizes
345 in the principal piece of flagella (Maruyama *et al.* 2016), the intracellular localization (and transport
346 substrates) of SLC22A14 is controversial. However, it is possible that pHi is affected by the
347 accumulation of these metabolites. Another possible cause of the impaired influx of HCO_3^- /low pHi
348 is that the expression or function of HCO_3^- or H^+ transporters are impaired in *Slc22a14* KO sperm. It
349 is widely recognized that three solute carrier transporter families—the SLC9 family (Na^+/H^+
350 exchanger), SLC4 family (bicarbonate transporter), and SLC26 family (multifunctional anion

351 transporter)—are involved in the regulation of pHi in somatic cells. In addition, cystic fibrosis
352 transmembrane conductance regulator (CFTR, an ABC type HCO₃⁻ transporter), the voltage-gated
353 hydrogen channel Hv1, and the Na-K-Cl cotransporter NKCC1 (also called SLC12A1) are also
354 involved in HCO₃⁻ transport and pHi regulation. Among them, *Slc4a4*, *Slc4a5*, and *Slc4a8* are
355 expressed in the testes at the mRNA or protein level (Pushkin *et al.* 2000, Grichtchenko *et al.* 2001,
356 Bernardino *et al.* 2013). SLC9A1 (NHE1), SLC9A5 (NHE5), SLC9A10 (sNHE), SLC9B1 (NHA1),
357 SLC9B2 (NHA2), SLC4A2 (AE2), SLC26A3, SLC26A6, SLC26A8 (TAT1), CFTR, Hv1, and
358 SLC12A1 are expressed in spermatozoa (Holappa *et al.* 1999, Woo *et al.* 2002, Toure *et al.* 2007,
359 Wang *et al.* 2007, Wertheimer *et al.* 2008, Lishko *et al.* 2010, Chávez *et al.* 2012, Figueiras-Fierro
360 *et al.* 2013, Chen *et al.* 2016). Therefore, decreased expression or function of these transporters/channels
361 could be a cause of impaired capacitation in *Slc22a14* KO sperm. We found that the protein expression
362 of SLC26A3, SLC26A6, SLC26A8, SLC9B1, and SLC9A10 in *Slc22a14* KO sperm was comparable
363 to that in WT sperm using western blotting or iTRAQ analysis. In addition, the expression of *Slc4a2*,
364 *Slc4a4*, *Slc4a5*, *Slc4a8*, *Slc9b2*, and *Slc12a1* did not decrease at the mRNA level. However, the protein
365 expression and functions of many candidate transporters in *Slc22a14* KO sperm could not be fully
366 determined. It will be necessary to analyze this in detail in the future.

367 Membrane fraction iTRAQ analysis revealed that 13 proteins were downregulated in
368 *Slc22a14* KO sperm. Among them, TMEM225, CEACAM10, and SVS5 are known or predicted to be
369 involved in sperm motility, capacitation, and male fertility. For example, TMEM225 is a possible
370 inhibitor of protein phosphatase 1 (PP1), which plays a critical role in sperm differentiation, motility,
371 and capacitation (Matsuura & Yogo 2015). CEACAM10 is a seminal vesicle secreted protein that
372 binds to the sperm membrane and enhances sperm motility (Li *et al.* 2005). Although the physiological
373 function of SVS5 has not been explored, the related family proteins SVS2, SVS3, and SVS4 act as
374 capacitation inhibitors or decapacitation factors (Araki *et al.* 2015, Araki *et al.* 2016). It is unclear why
375 the seminal vesicle proteins CEACAM10 and SVS5 were identified in cauda epididymal sperm, but

376 transcriptome data published in NCBI (<https://www.ncbi.nlm.nih.gov/gene/26366> and
377 <https://www.ncbi.nlm.nih.gov/gene/20944>) confirmed their expression in mouse testes, albeit at low
378 levels. Therefore, decreased expression of these proteins may be involved in the impairment of sperm
379 function and infertility in *Slc22a14* KO sperm. We confirmed the reduced expression of TMEM225
380 by western blotting and found that it was regulated by the translation level or protein degradation level.
381 Interestingly, IMPC recently described that *Tmem225* KO mice show male infertility. The cause and
382 molecular mechanism of male infertility in *Tmem225* KO mice remain unclear. The function of
383 TMEM225 in pHi regulation and capacitation needs to be assessed.

384 In conclusion, we investigated the mechanism of impaired capacitation in *Slc22a14* KO
385 mice and found that the influx of HCO_3^- and regulation of pHi were impaired. These results suggest
386 that HCO_3^- or H^+ transport is functionally related to organic ion transport. Our study provides
387 important insights into the molecular mechanisms of HCO_3^- influx and pHi regulation, which are
388 critical for sperm capacitation. Furthermore, we found that the addition of an alkalizing reagent and
389 cAMP can rescue decreased fertility in *Slc22a14* KO sperm. Because *Slc22a14* is a potential causative
390 gene for male infertility, our study provides a baseline technique that may be useful for therapeutic
391 purposes.

392

393

394 **Declaration of interest**

395 The authors declare that there are no conflicts of interest that could be perceived as prejudicing the
396 impartiality of the research reported.

397

398 **Funding**

399 This study was supported in part by the Ministry of Education, Culture, Sports, Science, and
400 Technology (MEXT) KAKENHI (Grant Number 18K06016).

401

402 **Author contribution statement**

403 Ito MO, Unou M, and Higuchi T performed the study. So S and Ito MA performed iTRAQ analysis
404 and contributed to the interpretation of the data. Yogo K designed and performed the experiments and
405 wrote the manuscript. All authors reviewed and approved the final manuscript.

406

407 **References**

- 408 Alasmari W, Costello S, Correia J, Oxenham SK, Morris J, Fernandes L, Ramalho-Santos J, Kirkman-
409 Brown J, Michelangeli F, Publicover S *et.al.* 2013 Ca²⁺ signals generated by CatSper and Ca²⁺
410 stores regulate different behaviors in human sperm. *J Biol Chem* **288** 6248-6258.
- 411 Araki N, Kawano N, Kang W, Miyado K, Yoshida K & Yoshida M 2016 Seminal vesicle proteins SVS3
412 and SVS4 facilitate SVS2 effect on sperm capacitation. *Reproduction* **152** 313-321.
- 413 Araki N, Trencsényi G, Krasznai ZT, Nizsalóczki E, Sakamoto A, Kawano N, Miyado K, Yoshida K &
414 Yoshida M 2015 Seminal vesicle secretion 2 acts as a protectant of sperm sterols and prevents
415 ectopic sperm capacitation in mice. *Biol Reprod* **92** 8.
- 416 Bernardino RL, Martins AD, Socorro S, Alves MG & Oliveira PF 2013 Effect of prediabetes on membrane
417 bicarbonate transporters in testis and epididymis. *J Membr Biol* **246** 877-883.
- 418 Chen SR, Chen M, Deng SL, Hao XX, Wang XX & Liu YX 2016 Sodium-hydrogen exchanger NHA1 and
419 NHA2 control sperm motility and male fertility. *Cell Death Dis* **7** e2152.
- 420 Chen Y, Cann MJ, Litvin TN, Iourgenko V, Sinclair ML, Levin LR & Buck J 2000 Soluble adenylyl cyclase
421 as an evolutionarily conserved bicarbonate sensor. *Science* **289** 625-628.
- 422 Chávez JC, Hernández-González EO, Wertheimer E, Visconti PE, Darszon A & Treviño CL 2012
423 Participation of the Cl⁻/HCO₃⁻ exchangers SLC26A3 and SLC26A6, the Cl⁻ channel CFTR, and
424 the regulatory factor SLC9A3R1 in mouse sperm capacitation. *Biol Reprod* **86** 1-14.
- 425 D'Amours O, Calvo E, Bourassa S, Vincent P, Blondin P & Sullivan R 2019 Proteomic markers of low and
426 high fertility bovine spermatozoa separated by Percoll gradient. *Mol Reprod Dev.*
- 427 Demarco IA, Espinosa F, Edwards J, Sosnik J, De La Vega-Beltran JL, Hockensmith JW, Kopf GS, Darszon
428 A & Visconti PE 2003 Involvement of a Na⁺/HCO₃⁻ cotransporter in mouse sperm capacitation.
429 *J Biol Chem* **278** 7001-7009.
- 430 Figueiras-Fierro D, Acevedo JJ, Martínez-López P, Escoffier J, Sepúlveda FV, Balderas E, Orta G, Visconti
431 PE & Darszon A 2013 Electrophysiological evidence for the presence of cystic fibrosis
432 transmembrane conductance regulator (CFTR) in mouse sperm. *J Cell Physiol* **228** 590-601.
- 433 Gadella BM 2008 Sperm membrane physiology and relevance for fertilization. *Anim Reprod Sci* **107** 229-
434 236.

435 Grichtchenko, II, Choi I, Zhong X, Bray-Ward P, Russell JM & Boron WF 2001 Cloning, characterization,
436 and chromosomal mapping of a human electroneutral Na(+)-driven Cl-HCO₃ exchanger. *J Biol*
437 *Chem* **276** 8358-8363.

438 Haan C & Behrmann I 2007 A cost effective non-commercial ECL-solution for Western blot detections
439 yielding strong signals and low background. *J Immunol Methods* **318** 11-19.

440 Holappa K, Mustonen M, Parvinen M, Vihko P, Rajaniemi H & Kellokumpu S 1999 Primary structure of a
441 sperm cell anion exchanger and its messenger ribonucleic acid expression during spermatogenesis.
442 *Biol Reprod* **61** 981-986.

443 Jaiswal BS & Conti M 2001 Identification and functional analysis of splice variants of the germ cell soluble
444 adenylyl cyclase. *J Biol Chem* **276** 31698-31708.

445 Kirichok Y, Navarro B & Clapham DE 2006 Whole-cell patch-clamp measurements of spermatozoa reveal
446 an alkaline-activated Ca²⁺ channel. *Nature* **439** 737-740.

447 Kuang W, Zhang J, Lan Z, Deepak R, Liu C, Ma Z, Cheng L, Zhao X, Meng X, Wang W *et. al.* 2021
448 SLC22A14 is a mitochondrial riboflavin transporter required for sperm oxidative phosphorylation
449 and male fertility. *Cell Rep* **35** 109025.

450 Li SH, Lee RK, Hsiao YL & Chen YH 2005 Demonstration of a glycoprotein derived from the Ceacam10
451 gene in mouse seminal vesicle secretions. *Biol Reprod* **73** 546-553.

452 Lishko PV, Botchkina IL, Fedorenko A & Kirichok Y 2010 Acid extrusion from human spermatozoa is
453 mediated by flagellar voltage-gated proton channel. *Cell* **140** 327-337.

454 Liu Y, Wang DK & Chen LM 2012 The physiology of bicarbonate transporters in mammalian reproduction.
455 *Biol Reprod* **86** 99.

456 Maruyama SY, Ito M, Ikami Y, Okitsu Y, Ito C, Toshimori K, Fujii W & Yogo K 2016 A critical role of
457 solute carrier 22a14 in sperm motility and male fertility in mice. *Sci Rep* **6** 36468.

458 Matsuura M & Yogo K 2015 TMEM225: a possible protein phosphatase 1gamma2 (PP1gamma2) regulator
459 localizes to the equatorial segment in mouse spermatozoa. *Mol Reprod Dev* **82** 139-148.

460 Muroi T, Matsushima Y, Kanamori R, Inoue H, Fujii W & Yogo K 2017 GPR62 constitutively activates
461 cAMP signaling but is dispensable for male fertility in mice. *Reproduction* **154** 755-764.

462 Nishigaki T, Jose O, Gonzalez-Cota AL, Romero F, Trevino CL & Darszon A 2014 Intracellular pH in
463 sperm physiology. *Biochem Biophys Res Commun* **450** 1149-1158.

464 Okamura N, Tajima Y, Soejima A, Masuda H & Sugita Y 1985 Sodium bicarbonate in seminal plasma
465 stimulates the motility of mammalian spermatozoa through direct activation of adenylate cyclase.
466 *J Biol Chem* **260** 9699-9705.

467 Pushkin A, Abuladze N, Newman D, Lee I, Xu G & Kurtz I 2000 Two C-terminal variants of NBC4, a new
468 member of the sodium bicarbonate cotransporter family: cloning, characterization, and
469 localization. *IUBMB Life* **50** 13-19.

470 Ren D, Navarro B, Perez G, Jackson AC, Hsu S, Shi Q, Tilly JL & Clapham DE 2001 A sperm ion channel
471 required for sperm motility and male fertility. *Nature* **413** 603-609.

472 Schneider CA, Rasband WS & Eliceiri KW 2012 NIH Image to ImageJ: 25 years of image analysis. *Nat*
473 *Methods* **9** 671-675.

474 Schreiber M, Wei A, Yuan A, Gaut J, Saito M & Salkoff L 1998 Slo3, a novel pH-sensitive K⁺ channel
475 from mammalian spermatocytes. *J Biol Chem* **273** 3509-3516.

476 Toure A, Lhuillier P, Gossen JA, Kuil CW, Lhote D, Jegou B, Escalier D & Gacon G 2007 The testis anion
477 transporter 1 (Slc26a8) is required for sperm terminal differentiation and male fertility in the
478 mouse. *Hum Mol Genet* **16** 1783-1793.

479 Visconti PE, Bailey JL, Moore GD, Pan D, Olds-Clarke P & Kopf GS 1995a Capacitation of mouse
480 spermatozoa. I. Correlation between the capacitation state and protein tyrosine phosphorylation.
481 *Development* **121** 1129-1137.

482 Visconti PE, Moore GD, Bailey JL, Leclerc P, Connors SA, Pan D, Olds-Clarke P & Kopf GS 1995b
483 Capacitation of mouse spermatozoa. II. Protein tyrosine phosphorylation and capacitation are
484 regulated by a cAMP-dependent pathway. *Development* **121** 1139-1150.

485 Wang D, Hu J, Bobulescu IA, Quill TA, McLeroy P, Moe OW & Garbers DL 2007 A sperm-specific
486 Na⁺/H⁺ exchanger (sNHE) is critical for expression and in vivo bicarbonate regulation of the
487 soluble adenylyl cyclase (sAC). *Proc Natl Acad Sci U S A* **104** 9325-9330.

488 Wertheimer EV, Salicioni AM, Liu W, Trevino CL, Chavez J, Hernández-González EO, Darszon A &
489 Visconti PE 2008 Chloride is essential for capacitation and for the capacitation-associated increase
490 in tyrosine phosphorylation. *J Biol Chem* **283** 35539-35550.

491 Woo AL, James PF & Lingrel JB 2002 Roles of the Na,K-ATPase alpha4 isoform and the Na⁺/H⁺
492 exchanger in sperm motility. *Mol Reprod Dev* **62** 348-356.

493 Zeng XH, Yang C, Kim ST, Lingle CJ & Xia XM 2011 Deletion of the Slo3 gene abolishes alkalization-
494 activated K⁺ current in mouse spermatozoa. *Proc Natl Acad Sci U S A* **108** 5879-5884.

495

496

497 **Figure legends**

498

499 Figure 1. Impaired capacitation in *Slc22a14* KO mouse sperm

500 A) Wild-type (WT) and *Slc22a14* KO (KO) mouse sperm were incubated for the indicated times.

501 Protein tyrosine phosphorylation levels were monitored by western blotting using anti-phospho-

502 tyrosine antibody (p-Tyr). Anti-GAPDH antibody was used to monitor the amount of protein loaded.

503 Lysate equivalent to 5×10^5 sperm was loaded per 1 lane. Experiments were performed independently

504 three times, and the representative result are shown here. B) Quantification of protein tyrosine

505 phosphorylation level. The signals of the bands marked with an asterisk were quantified and

506 normalized to the corresponding amount of GAPDH. The values were indicated as a ratio to

507 maximum intensity \pm SEM ($n = 3$). The results that vary significantly, according to Tukey's multiple

508 comparison test, are indicated with different letters ($p < 0.05$).

509

510 Figure 2. Reduced capacitation-associated cAMP production in *Slc22a14* KO sperm

511 Intracellular cAMP concentration during capacitation in wild-type (closed circles) and *Slc22a14* KO

512 mouse sperm (open circles). Data are presented as the mean \pm SEM ($n = 4$). The results that vary

513 significantly, according to Tukey's multiple comparison test, are indicated with different letters (p

514 < 0.05).

515

516 Figure 3. Normal HCO_3^- -dependent soluble adenylyl cyclase activity in *Slc22a14* KO sperm

517 Adenylyl cyclase activity was measured in the presence or absence of HCO_3^- using a cytosolic

518 fraction of wild-type (WT) and *Slc22a14* KO (KO) sperm. The activity of *Slc22a14* KO sperm was

519 comparable to that of WT sperm. Data are presented as the mean \pm SEM ($n = 4$).

520

521 Figure 4. Cell-permeable cAMP rescues impaired capacitation in *Slc22a14* KO sperm

522 A) Wild-type and KO mouse sperm were incubated in the presence or absence of 8-bromo cAMP
523 (0.5 mM) and IBMX (50 μ M) for 60 min. Protein tyrosine phosphorylation was monitored by
524 western blotting. Lysate equivalent to 5×10^5 sperm was loaded per 1 lane. B) Quantification of
525 protein tyrosine phosphorylation level. The signals of the bands marked with an asterisk in panel A
526 were quantified as shown in Fig. 1, and the relative intensities to the value of wild-type cAMP (-)
527 group were calculated. Data are presented as the mean \pm SEM ($n = 3$). The results that vary
528 significantly, according to Tukey's multiple comparison test, are indicated with different letters (p
529 < 0.05).

530

531 Figure 5. Impaired influx of HCO_3^- in *Slc22a14* KO sperm

532 The intracellular pH of wild-type and KO mouse sperm during incubation was measured using
533 BCECF-AM. Data are presented as the mean \pm SEM ($n = 3$). The results that vary significantly,
534 according to Tukey's multiple comparison test, are indicated with different letters ($p < 0.05$).

535

536 Figure 6. Expression of TMEM225 in the *Slc22a14* KO testis

537 A) Expression of TMEM225 in wild-type and KO testes was detected by western blotting. Three
538 individual mice were used in each group. We performed immunoprecipitation (IP)-western blotting
539 with anti-TMEM225 antibody. To confirm that equal amounts of protein were used for IP, whole cell
540 lysate (4 μ g) were loaded and blotted with anti-GAPDH antibody. B) Relative expression level of
541 TMEM225 in *Slc22a14* KO testis. The signal intensity of TMEM225 were quantified and
542 normalized to that of GAPDH. The values are presented as average \pm SEM ($n = 3$). C) Gene
543 expression of *Tmem225* in the wild-type and KO testis were analyzed with semi-quantitative RT-
544 PCR. The number indicate the number of cycles of PCR. Data representative of two independent
545 experiments are shown.

546

547 Figure 7. Addition of trimethylamine and cAMP partially rescued the decreased fertilization rate in
548 *Slc22a14* KO sperm
549 A) Effect of trimethylamine and cAMP/IBMX on in vitro fertilization rate. WT and KO mouse
550 sperm were incubated in TYH medium supplemented with the indicated reagents (TMA, 10 mM
551 trimethylamine; cAMP, 0.5 mM 8-bromo cAMP and 50 μ M IBMX) for 60 min and incubated with
552 WT oocytes. The percentage of 2-cell embryos was counted 24 h after insemination. B) Effect of
553 TMA and cAMP/IBMX on sperm morphology. Sperm were incubated in each experimental
554 condition for 60 min; then, they were individually classified based on whether they had normal
555 morphology or abnormal flagellar bending and counted. C) Effect of TMA and cAMP/IBMX on
556 sperm motility. Sperm were incubated in each experimental condition for 60 min and sperm motility
557 was observed under the microscope. The percentage of sperm in three motility categories (highly
558 motile, motile, and immotile) was determined.

559

560 **Supplementary Figure legends**

561 Figure S1. Expression of HCO₃⁻ and H⁺ transporter in *Slc22a14* KO mouse testis

562 A) Expression of indicated transporters in testes were analyzed by semi-quantitative PCR. The
563 numbers above the photo indicate the PCR cycles. The band indicated with an asterisk in *Slc9a10*
564 may be a splicing isoform. Data representative of two independent experiments are shown. B) The
565 western blotting analysis of SLC26A3 and SLC26A6 in WT and *Slc22a14* KO sperm. Data
566 representative of two independent experiments are shown.

567

568 Figure S2. iTRAQ analysis using total cell lysate of sperm

569 A) The abundance of protein in WT and KO sperm are plotted. Almost of all protein shows similar
570 expression level. B) Top 10 protein list downregulated in *Slc22a14* KO sperm.

571

572 Figure S3. Effect of trimethylamine on pHi of sperm
573 BCECF-loaded WT and KO sperm were incubated in TYH-HEPES medium supplemented with
574 25.07 mM NaHCO₃, 4 mg/ml BSA, and the indicated concentration of trimethylamine (TMA) for 30
575 min, and pHi was measured using a spectrophotometer.

Table 1. Downregulated proteins in *Slc22a14* KO sperm

UniProt Accession	Protein Name	Sum PEP Score	Coverage	MW [kDa]	Entrez Gene ID	Abundance Ratio (KO/WT)
Q9D9S2	Transmembrane protein 225	4.8	5.2	26.5	Tmem225	0.274
Q30D77	Collagen alpha-1(XXIV) chain	1.2	0.5	175.6	Col24a1	0.308
P30933	Seminal vesicle secretory protein 5	12.7	23.0	13	Svs5	0.323
Q9QZ29	Immunoglobulin-binding protein 1b	3.0	3.5	39.2	Igpb1b	0.350
P70195	Proteasome subunit beta type-7	17.5	14.5	45.6	Psmb7	0.402
P62196	26S proteasome regulatory subunit 8	11.4	7.2	29.9	Psmc5	0.403
Q61400	Carcinoembryonic antigen-related cell adhesion molecule 10	5.0	6.4	29.5	Ceacam10	0.422
Q8C5W0	Calmin	8.7	3.0	117.2	Clmn	0.466
Q9Z1Q9	Valine--tRNA ligase	6.7	4.6	25.4	Vars	0.469
Q60692	Proteasome subunit beta type-6	4.7	0.8	140.1	Psmb6	0.487
Q9D8W5	26S proteasome non-ATPase regulatory subunit 12	12.1	9.4	52.9	Psm12	0.489
P22892	AP-1 complex subunit gamma-1	56.9	32.1	52.2	Ap1g1	0.496
Q9Z2W0	Aspartyl aminopeptidase	4.8	5.2	26.5	Dnpep	0.497

Membrane fractions of sperm of wild-type and *Slc22a14* KO sperm were extracted and differential protein expression was analyzed using iTRAQ technology. Only the proteins that changed by two-fold or more are shown. No protein was identified as upregulated in KO sperm. Posterior Error Probabilities (PEP) score indicates the confidence of individual Peptide Sequence Matches.

Table 2. SLC transporters identified by iTRAQ analysis

UniProt Accession	Protein Name	Sum PEP Score	Coverage	MW [kDa]	Entrez Gene ID	Abundance Ratio (KO/WT)
Q9WTN6	Solute carrier family 22 member 21	23.4	9.4	63.3	Slc22a21	0.815
Q8R0C3	Testis anion transporter 1	12.1	3.4	112.9	Slc26a8	0.825
P32037	Solute carrier family 2, facilitated glucose transporter member 3	189.1	18.3	53.4	Slc2a3	0.840
Q60738	Zinc transporter 1	6.2	3.8	54.7	Slc30a1	0.852
Q8K596	Sodium/calcium exchanger 2	19.0	6.9	100.6	Slc8a2	0.897
Q8C0X2	Sodium/hydrogen exchanger 9B1	52.8	15.0	61.9	Nhedc1; Slc9b1	0.904
Q9WV38	Solute carrier family 2, facilitated glucose transporter member 5	52.1	12.2	55.4	Slc2a5	0.917
O70451	Monocarboxylate transporter 2	41.5	17.8	52.6	Slc16a7	0.935
P10852	4F2 cell-surface antigen heavy chain	4.3	4.0	58.3	Slc3a2	0.955
Q8BH59	Calcium-binding mitochondrial carrier protein Aralar1	7.0	7.4	74.5	Slc25a12	0.976
Q6UJY2	Sodium/hydrogen exchanger 10	2.2	1.3	135.5	Slc9a10; Slc9c1	1.004
Q497L8	Solute carrier family 22 member 16	5.9	1.8	73.9	Slc22a16	1.058
Q8VEM8	Phosphate carrier protein, mitochondrial	23.8	14.6	39.6	Slc25a3	1.106
P31650	Sodium- and chloride-dependent GABA transporter 3	3.2	1.4	69.9	Slc6a11	1.118
Q3V132	ADP/ATP translocase 4	97.4	48.8	35.2	Slc25a31	1.119
P48962	ADP/ATP translocase 1	45.8	31.2	32.9	Slc25a4	1.137

Q7TML3	Solute carrier family 35 member F2	1.9	2.1	41.6	Slc35f2	1.153
P51881	ADP/ATP translocase 2	8.9	5.0	31	Slc25a5	1.187
P53986	Monocarboxylate transporter 1	14.0	6.7	53.2	Slc16a1	1.226

Transporters shown in bold are involved in the regulation of pHi in sperm.

Figure 1

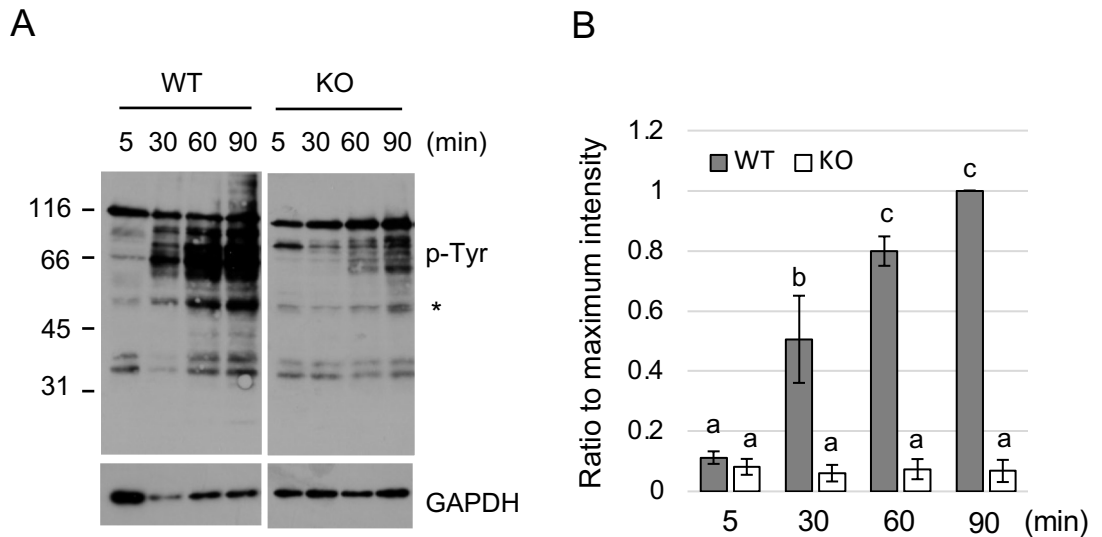


Figure 1. Impaired capacitation in *Slc22a14* KO mouse sperm

A) Wild-type (WT) and *Slc22a14* KO (KO) mouse sperm were incubated for the indicated times. Protein tyrosine phosphorylation levels were monitored by western blotting using anti-phospho-tyrosine antibody (p-Tyr). Anti-GAPDH antibody was used to monitor the amount of protein loaded. Lysate equivalent to 5×10^5 sperm was loaded per 1 lane. Experiments were performed independently three times, and the representative result are shown here. B) Quantification of protein tyrosine phosphorylation level. The signals of the bands marked with an asterisk were quantified and normalized to the corresponding amount of GAPDH. The values were indicated as a ratio to maximum intensity \pm SEM ($n = 3$). The results that vary significantly, according to Tukey's multiple comparison test, are indicated with different letters ($p < 0.05$).

Figure 2

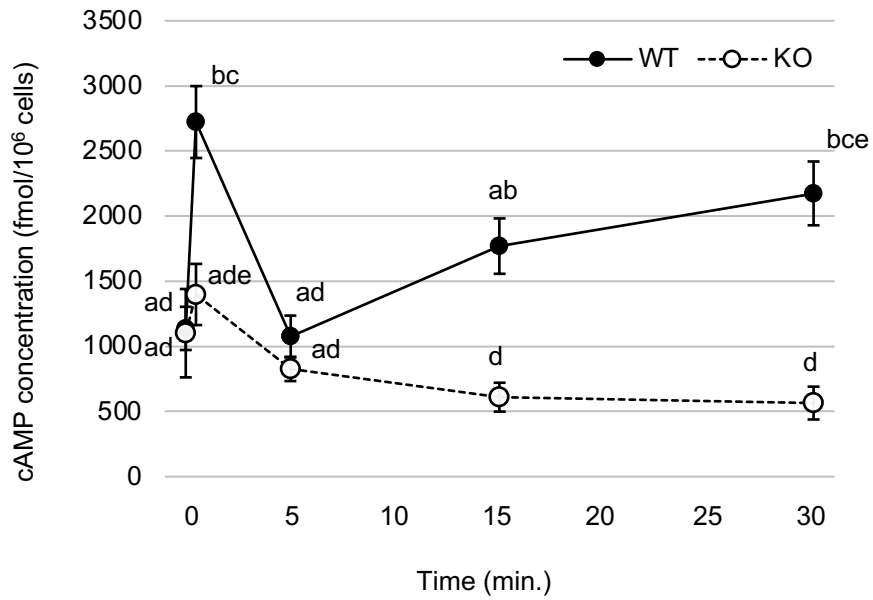


Figure 2. Reduced capacitation-associated cAMP production in *Slc22a14* KO sperm
Intracellular cAMP concentration during capacitation in wild-type (closed circles) and *Slc22a14* KO mouse sperm (open circles). Data are presented as the mean \pm SEM ($n = 4$). The results that vary significantly, according to Tukey's multiple comparison test, are indicated with different letters ($p < 0.05$).

Figure 3

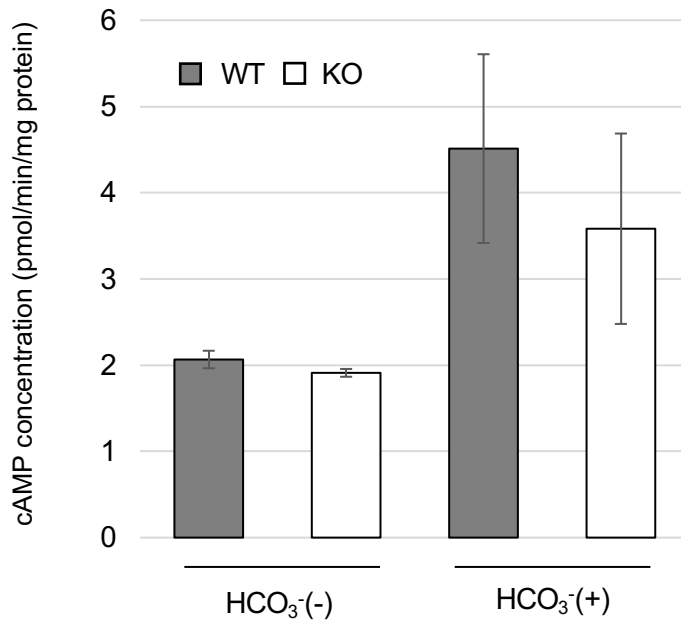


Figure 3. Normal HCO₃⁻-dependent soluble adenylyl cyclase activity in *Slc22a14* KO sperm

Adenylyl cyclase activity was measured in the presence or absence of HCO₃⁻ using a cytosolic fraction of wild-type (WT) and *Slc22a14* KO (KO) sperm. The activity of *Slc22a14* KO sperm was comparable to that of WT sperm. Data are presented as the mean ± SEM ($n = 4$).

Figure 4

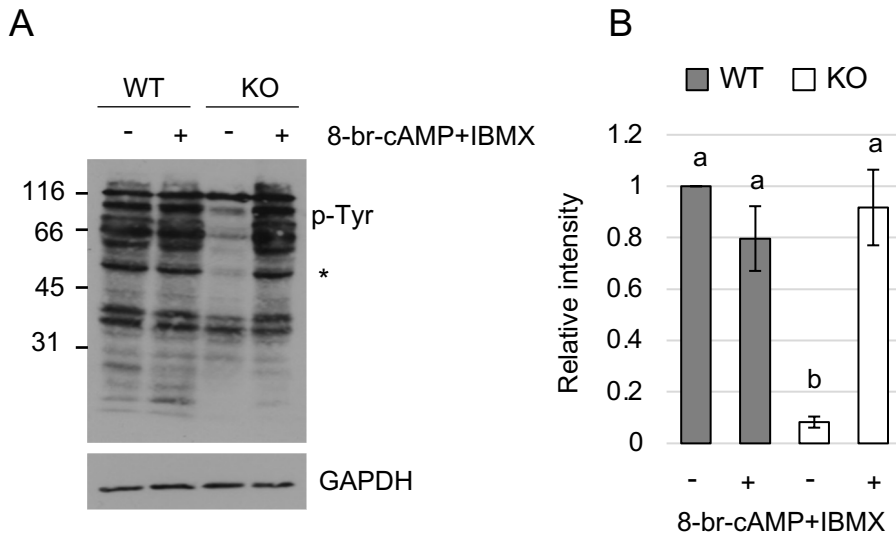


Figure 4. Cell-permeable cAMP rescues impaired capacitation in *Slc22a14* KO sperm
A) Wild-type and KO mouse sperm were incubated in the presence or absence of 8-bromo cAMP (0.5 mM) and IBMX (50 μ M) for 60 min. Protein tyrosine phosphorylation was monitored by western blotting. Lysate equivalent to 5×10^5 sperm was loaded per 1 lane. B) Quantification of protein tyrosine phosphorylation level. The signals of the bands marked with an asterisk in panel A were quantified as shown in Fig. 1, and the relative intensities to the value of wild-type cAMP (-) group were calculated. Data are presented as the mean \pm SEM ($n = 3$). The results that vary significantly, according to Tukey's multiple comparison test, are indicated with different letters ($p < 0.05$).

Figure 5

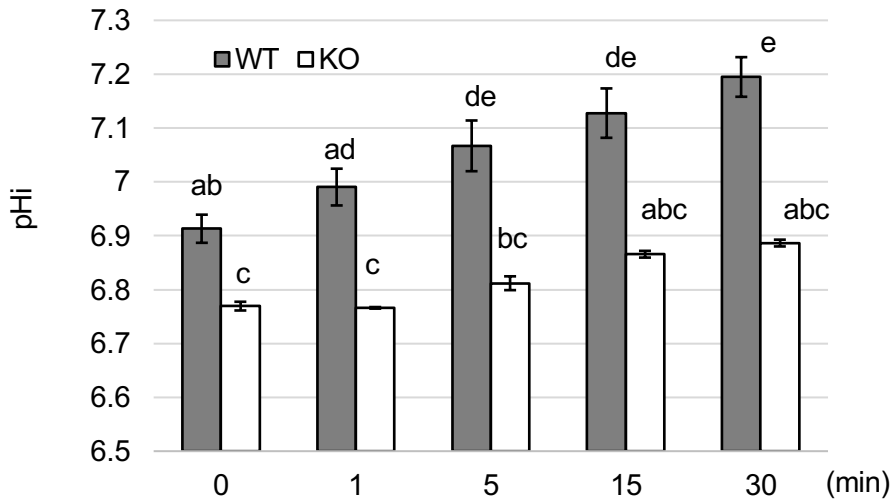


Figure 5. Impaired influx of HCO_3^- in *Slc22a14* KO sperm

The intracellular pH of wild-type and KO mouse sperm during incubation was measured using BCECF-AM. Data are presented as the mean \pm SEM ($n = 3$).

The results that vary significantly, according to Tukey's multiple comparison test, are indicated with different letters ($p < 0.05$).

Figure 6

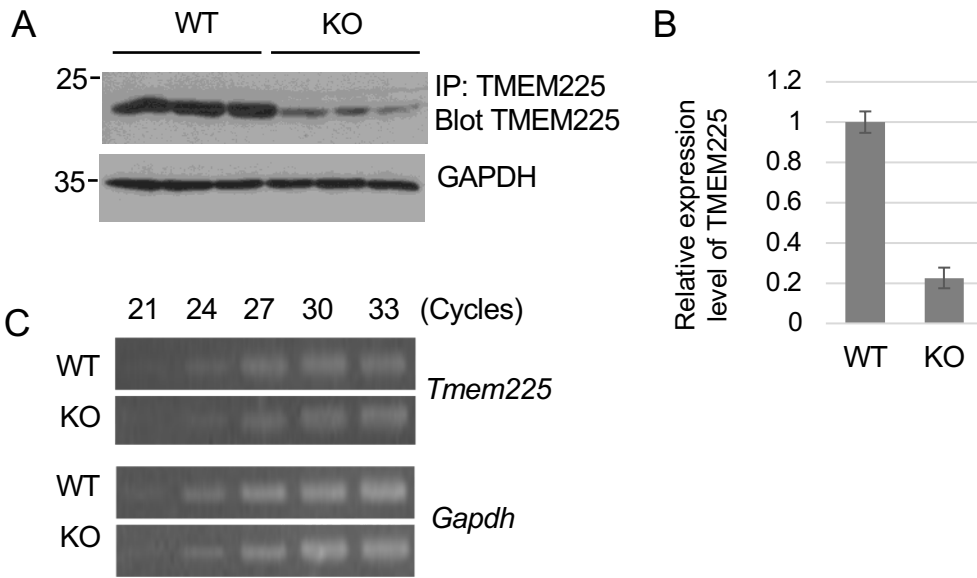


Figure 6. Expression of TMEM225 in the *Slc22a14* KO testis

A) Expression of TMEM225 in wild-type and KO testes was detected by western blotting. Three individual mice were used in each group. We performed immunoprecipitation (IP)-western blotting with anti-TMEM225 antibody. To confirm that equal amounts of protein were used for IP, whole cell lysate (4 μ g) were loaded and blotted with anti-GAPDH antibody. B) Relative expression level of TMEM225 in *Slc22a14* KO testis. The signal intensity of TMEM225 were quantified and normalized to that of GAPDH. The values are presented as average \pm SEM ($n = 3$). C) Gene expression of *Tmem225* in the wild-type and KO testis were analyzed with semi-quantitative RT-PCR. The number indicate the number of cycles of PCR. Data representative of two independent experiments are shown.

Figure 7

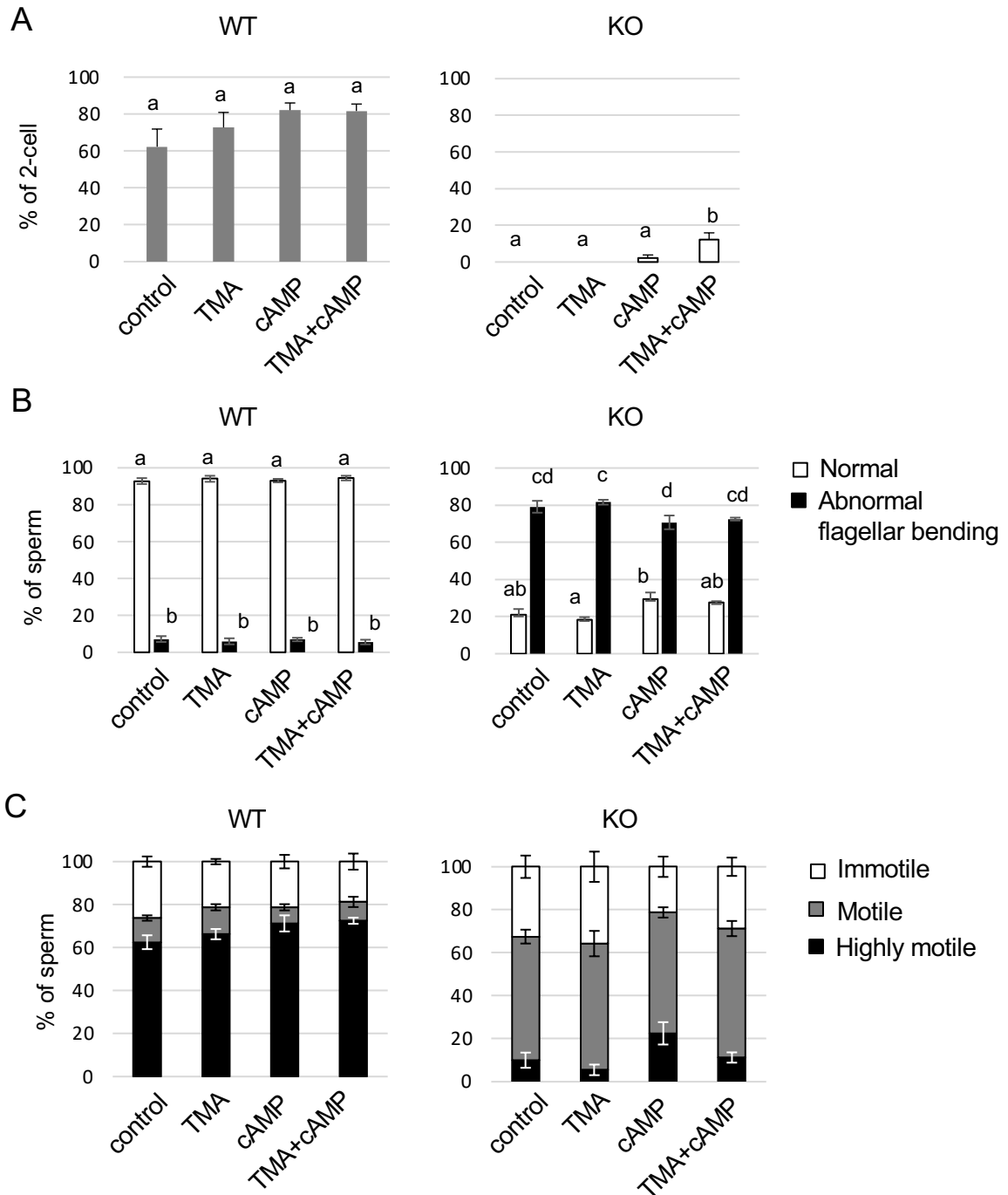


Figure 7. Addition of trimethylamine and cAMP partially rescued the decreased fertilization rate in *Slc22a14* KO sperm

A) Effect of trimethylamine and cAMP/IBMX on in vitro fertilization rate. WT and KO mouse sperm were incubated in TYH medium supplemented with the indicated reagents (TMA, 10 mM trimethylamine; cAMP, 0.5 mM 8-bromo cAMP and 50 μ M IBMX) for 60 min and incubated with WT oocytes. The percentage of 2-cell embryos was counted 24 h after insemination. B) Effect of TMA and cAMP/IBMX on sperm morphology. Sperm were incubated in each experimental condition for 60 min; then, they were individually classified based on whether they had normal morphology or abnormal flagellar bending and counted. C) Effect of TMA and cAMP/IBMX on sperm motility. Sperm were incubated in each experimental condition for 60 min and sperm motility was observed under the microscope. The percentage of sperm in three motility categories (highly motile, motile, and immotile) was determined.

Supplementary Table 1

Primer pairs and PCR condition used in semi-quantitative RT-PCR

Target	Sequence	Program
<i>Slc4a2</i>	5'- TGCCAAAGGGTCTACACAGGC -3' 5'- TCTGCTGATCGAGGTCTAAGAGC -3'	94°C for 2 min; 27-36 cycles of 98°C for 10 s, 60°C for 30 s, 68°C for 20 s.
<i>Slc4a4</i>	5'- TACTCACTTCTCTTGTGCTTGCCCTG -3' 5'- GCTGTGGTTGGAAAATAGCGACTG -3'	94°C for 2 min; 30-39 cycles of 98°C for 10 s, 60°C for 30 s, 68°C for 20 s.
<i>Slc4a5</i>	5'- GCACCAGCTATGGTCATCT -3' 5'- GCAGACTGGACAAGACGAACAAATG -3'	94°C for 2 min; 24-33 cycles of 98°C for 10 s, 60°C for 30 s, 68°C for 20 s.
<i>Slc4a8</i>	5'- ACCCATCTATTAGAATTGAGCCACC -3' 5'- TATGCGTCCTTCAGTGGCTTCTC -3'	94°C for 2 min; 27-36 cycles of 98°C for 10 s, 60°C for 30 s, 68°C for 20 s.
<i>Slc9b1</i>	5'- GCTTCCTAGAAGCCTGCTCAGC -3' 5'- CCCAATAAGAACGTCCCGCAAG -3'	94°C for 2 min; 24-33 cycles of 98°C for 10 s, 60°C for 30 s, 68°C for 20 s.
<i>Slc9b2</i>	5'- AAGTTTCCAACATTGCCTCCTCTG -3' 5'- CTACGACAAAACCCAGGATGAACC -3'	94°C for 2 min; 24-33 cycles of 98°C for 10 s, 60°C for 30 s, 68°C for 20 s.
<i>Slc9a10</i>	5'- TTCAGATCCTATGCTTACTTCAGCC -3' 5'- AGAAGATGAGAGTGATGTGGTTGAC -3'	94°C for 2 min; 27-39 cycles of 98°C for 10 s, 60°C for 30 s, 68°C for 20 s.
<i>Slc12a1</i>	5'- AAGGCACGATTGATGTTTGGTGGT -3' 5'- AGTGTTCCCTGTAAGAGCTCGTTCAG -3'	94°C for 2 min; 27-36 cycles of 98°C for 10 s, 68°C for 30 s.
<i>Tmem225</i>	5'- GCTGCCAACATATTCTTCTCCTCTG -3' 5'- GAAGATACCTGCGAAGAACTCAGG -3'	94°C for 2 min; 21-33 cycles of 98°C for 10 s, 60°C for 30 s, 68°C for 20 s.
<i>Gapdh</i>	5'- CATCACCATCTTCCAGGAGCG -3' 5'- AAGGCCATGCCAGTGAGCTTC -3'	94°C for 2 min; 21-30 cycles of 98°C for 10 s, 60°C for 30 s, 68°C for 40 s.

Supplementary figure 1

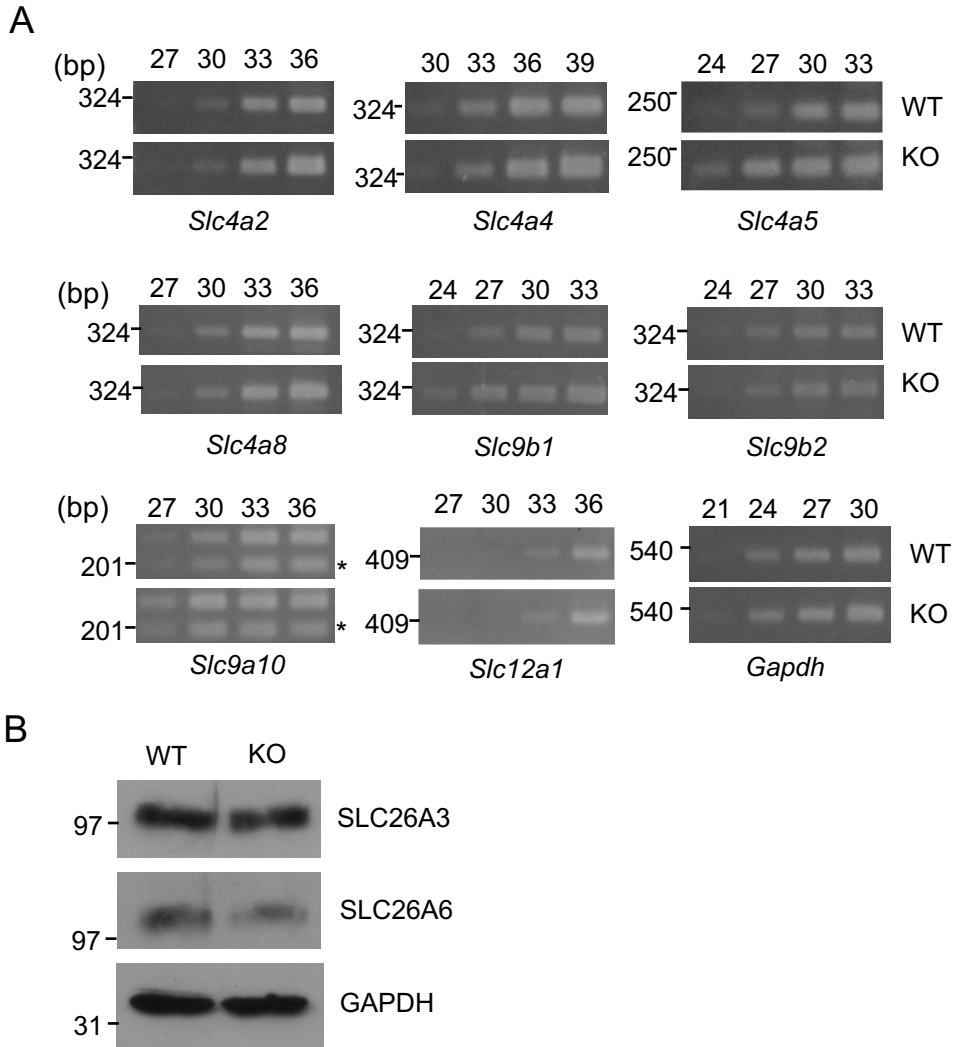
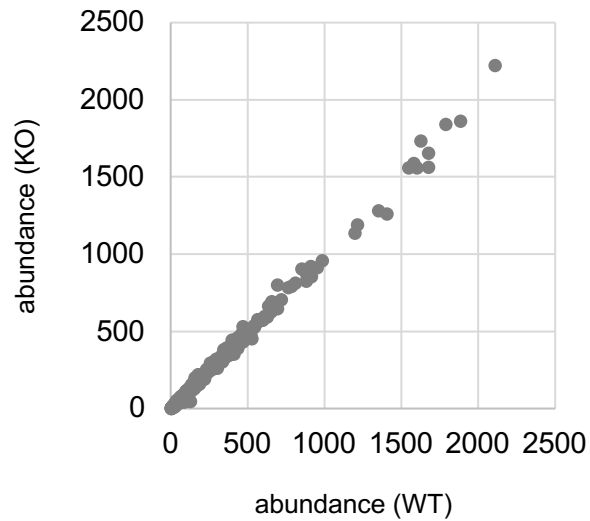


Figure S1. Expression of HCO_3^- and H^+ transporter in *Slc22a14* KO mouse testis
 A) Expression of indicated transporters in testes were analyzed by semi-quantitative PCR. The numbers above the photo indicate the PCR cycles. The band indicated with an asterisk in *Slc9a10* may be a splicing isoform. Data representative of two independent experiments are shown. B) The western blotting analysis of SLC26A3 and SLC26A6 in WT and *Slc22a14* KO sperm. Data representative of two independent experiments are shown.

Supplementary figure 2

A



B

Protein name	Abundance ratio (WT/KO)
Myosin, light polypeptide 6B	0.37
myosin, light polypeptide 1	0.51
Tropomyosin 1, alpha	0.514
RIKEN cDNA 1700001O22 gene	0.586
tubulin, beta 3 class III	0.655
Cytochrome c oxidase subunit VIIa 2	0.678
Sjogren syndrome antigen B	0.698
desmin	0.701
TSC22 domain family, member 4	0.733
tripeptidyl peptidase I	0.766

Figure S2. iTRAQ analysis using total cell lysate of sperm

A) The abundance of protein in WT and KO sperm are plotted. Almost of all protein shows similar expression level. B) Top 10 protein list downregulated in *Slc22a14* KO sperm.

Supplementary figure 3

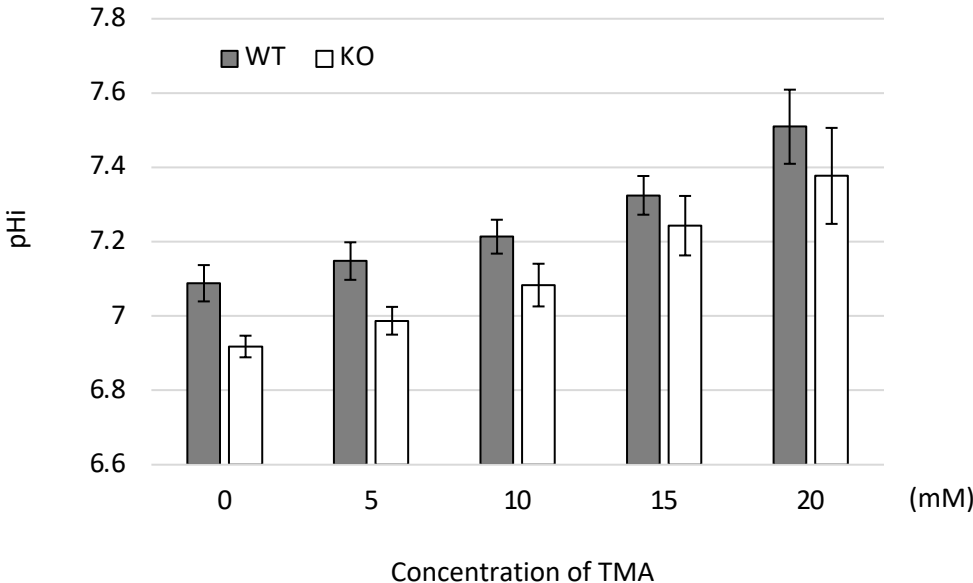


Figure S3. Effect of trimethylamine on pHi of sperm
BCECF-loaded WT and KO sperm were incubated in TYH-HEPES medium supplemented with 25.07 mM NaHCO₃, 4 mg/ml BSA, and the indicated concentration of trimethylamine (TMA) for 30 min, and pHi was measured using a spectrophotometer.